

Fracture driven by a Thermal Gradient

Oscar Pla*

*Instituto de Ciencia de Materiales, C.S.I.C.,
Universidad Autónoma de Madrid C-III, E-28049 Madrid, Spain.*

Abstract

Motivated by recent experiments by Yuse and Sano (*Nature*, **362**, 329 (1993)), we propose a discrete model of linear springs for studying fracture in thin and elastically isotropic brittle films. The method enables us to draw a map of the stresses in the material. Cracks generated by the model, imposing a moving thermal gradient in the material, can branch or wiggle depending on the driving parameters. The results may be used to compare with other recent theoretical work, or to design future experiments.

PACS numbers: 62.20.Mk, 65.70.+y

arXiv:mtrl-th/9505005v1 12 May 1995

I. INTRODUCTION.

The study of brittle fracture is of particular technological interest for understanding the properties of ceramic materials. By *ceramic* we understand covalent ionic materials, including also glasses, polycrystalline aggregates, minerals and even composites [1]. Studies in the statistical physics and engineering aspects of the problem [2,3] have been carried out, and though some proposals have been made, a comprehensive and general understanding of the mechanisms leading to fracture is still missing. The fundamental reason for this apparent lack of progress may be that experimental work in the study of these processes is very difficult because of the great quantity of parameters that seem to have impact in the resulting shape or velocity of the crack. Recently Yuse and Sano carried out an experiment [4] in which they could control the fracture pattern as function of the external imposed stresses. It is sketched in Fig. 1. A thin rectangular plate of glass with an initial notch is pulled at a velocity v inside a region of width 2ξ , where there is a change in the temperature from T_h to T_c . As function of increasing v , and also $\Delta T = T_h - T_c$, several phases may be found: first, for low values of the control parameters, no fracture is propagated. If the control parameter, i.e. v , is increased, a straight crack is generated. If it is again increased, a wiggling pattern similar to that of Fig. 1 appears. And, finally, for high enough values of v branching occurs, and more than one crack propagates in the system.

This experiment has inspired directly analytical [5,6] as well as numerical [7,8] work. Recent numerical simulations [9] also show this oscillatory instability when the system is driven, not by a thermal gradient, but by an increasing strain in the borders.

The purpose of this paper is to introduce a discrete model that has the right long wave behavior of the continuum elasticity theory, and to check its predictions of wiggling cracks in the case of a thermally driven fracture. Here I will thus try to present the tool. Quantitative comparisons against analytical models and experiment will be the subject of future publications.

The basic physical ideas that inspire the model developed here are that brittle materials are elastic, in the strict sense that displacements are proportional to applied stresses, until they fail. Also, since the velocity of the crack propagation is imposed by the motion of the temperature change, and it is much smaller than the sound velocity in the material, quasistatic calculations are good candidates to give a right description of the problem.

In section II I will describe the model, expose the fracture processes, and see how the model reproduces qualitatively the thermally driven fracture scenario. In section III I will show how the stress profiles in the system can be calculated. Section IV will be dedicated to study the dependence of the different parameters when we want to produce larger systems (or better discretizations). Finally, in section V, we will present some conclusions and paths for future works and applications of the model.

II. MODEL AND SIMULATIONS.

A. Discretization.

The continuum elastic description of a two dimensional material that is in the presence of a temperature field, T , is given by the free energy [10]

$$\mathcal{F}_e = \frac{1}{2}(\lambda + \mu)(\varepsilon_{xx} + \varepsilon_{yy})^2 + \mu(2\varepsilon_{xy}^2 + \frac{1}{2}(\varepsilon_{xx} - \varepsilon_{yy})^2) - (\lambda + \mu)\alpha T(\varepsilon_{xx} + \varepsilon_{yy}), \quad (1)$$

where $\varepsilon_{ij} = (\partial_i u_j + \partial_j u_i)/2$ are the components of the strain tensor (u_i are the local deformations of the material in the i direction), λ and μ the Lamé coefficients, and α the thermal expansion.

As simple microscopic model we can consider a system of hookean springs described by the free energy

$$\mathcal{F}_s = \frac{1}{2} \sum_{ij} k_{ij} [(\mathbf{u}_j - \mathbf{u}_i) \cdot \hat{r}_{ij}]^2 - \sum_{ij} k_{ij} W_i (\mathbf{u}_j - \mathbf{u}_i) \cdot \hat{r}_{ij}, \quad (2)$$

where \mathbf{u}_i is the displacement of node i from its equilibrium position, \hat{r}_{ij} is the unitary vector that points from node i to node j , k_{ij} is the force constant of the spring that joins i th and j th nodes, and W_i is the scalar field that includes temperature, compression modulus, and thermal expansion at node i [11]. If the nodes are placed in a triangular lattice, and links are made all with the same force constant and only between nearest neighbors, the long wavelength behavior of Eq. 2 is the same as that described by the continuum Eq. 1, when the temperature is constant in the material, and with $\lambda = \mu$.

Let us introduce a reference system in terms of the axis of the triangular lattice, making the following changes of variables: $u = (2/\sqrt{3})x$ and $v = y + (1/\sqrt{3})x$ for the coordinates, and $u_u = (\sqrt{3}/2)u_x - (1/2)u_y$, $u_v = u_y$, and $u_w = u_u + u_v$ for the three vector displacements in the triangular lattice [12]. We will also take the vectors \hat{r}_{ij} as vectors in the triangular lattice, making the equations of motion linear in the displacements.

The free energy of the model can be written as

$$\mathcal{F}_s = \frac{1}{2} \sum_n \left((\partial_u u_u)^2 + (\partial_v u_v)^2 + (\partial_w u_w)^2 \right) - 2 \sum_n W_n (\partial_u u_u + \partial_v u_v + \partial_w u_w), \quad (3)$$

where n now sweeps all the nodes in the system, and the derivatives are evaluated as differences between neighbor nodes when there are links between them (k_{ij} takes values 0 (1) for missing (present) springs).

B. Temperature.

If the temperature drop is being displaced at a velocity v in the y direction, the thermal diffusion equation

$$\frac{\partial T}{\partial t} = \kappa \nabla^2 T, \quad (4)$$

accepts solutions that depend only on $\psi = y - vt$ in the form:

$$T(\psi) = \frac{T_h - T_c}{2} + \frac{T_h + T_c}{2} \frac{\cosh v\xi - \exp v\psi}{\sinh v\xi}, \quad (5)$$

where $v \equiv v/\kappa$ is the inverse of the temperature length, and 2ξ is the distance between the hot and the cold temperature baths. Function T is also sketched in Fig. 1. Notice that its derivative is not continuous at $T = T_c$, where the fastest changes in T are found, and, for that reason, larger stresses are located.

C. Initial conditions and relaxation.

To perform a simulation the nodes are placed in a rombus of dimensions $N_u \times N_v$, in units of the node-node distance. Then the corners are cut to make a rectangular sample of dimensions $(\sqrt{3}/2)N_u \times N_v - N_u/2$. A small notch cutting bonds at the edge simulate the experimental initial conditions. Now the temperature drop is introduced by applying W , following Eq. 5, with $y_0 \equiv vt$ far bellow the system. The set of nodes displacements, $\{u\}$, is then relaxed by the Conjugate Gradients Method [13] until forces (elastic and thermal) at each node are balanced.

D. Fracture.

Once the system is relaxed, springs whose stress (including difference in displacements and average W in the connected nodes) is more than some threshold value, σ_{th} , are allowed to break. Since pure deterministic breakdown can give rise to problems in the decision of which spring to break [7], we will make use of probabilistic breakdown following Louis and Guinea model [14], and considering four neighbors of the already broken springs [15]. In this model each spring has a probability of breaking proportional to a power η of its stress. If η is large enough (I will take in this work $\eta=10$), the method is, for all practical purposes, deterministic, except in those cases close to branching where there are two or several paths to which fracture may develop. If after the relaxation there are no springs with stresses larger than the threshold, the temperature field is displaced in the positive y -direction, $y_0 \rightarrow y_0 + \Delta y$, and the system is relaxed again. If breakdown occurs, the system is also relaxed without the broken bond and stresses recalculated without moving the temperature profile. The simulation stops when the crack gets close to the upper limit of the system.

E. Results.

As discussed in previously developed discrete models [7], the different shapes of cracks do not depend on the values of W_h and W_c , but on its difference, ΔW . In particular, the model presented here, as compression or dilation generate the same stressed state, depends only on the absolute value of ΔW . The units of ΔW are the same as σ_{th} , and properties are only dependent on $\Delta W/\sigma_{th}$. We will thus set $\sigma_{th} = 1$, and discuss its possible changes in section IV.

Several simulations with $\xi = 6$, and system size 30×100 are shown in Fig. 2. The model reproduces qualitatively well the phenomenology of thermally driven fracture described in section I. In Fig. 2 can be found several interesting configurations, ranging from branching in the middle of the plate, some time after the crack seems to be a wiggling one, to situations in which wiggling and straight cracks run parallel. In fact, it seems that, with enough CPU time, besides the line transitions from straight to wiggling, and from wiggling to branching, a line transition can be defined for any branching level, or even for transitions from two straight cracks to one wiggling and one straight.

This model has not the invariance reported in Ref. [7] with respect of width- v , or, in other words, that the effective thermal lenght, sets the units of the width of the system. This is not

the case here because we have considered another parameter, that is, the distance between the two applied temperature baths, 2ξ . As a consequence, the temperature as function of distance is an exponential and not an hyperbolic tangent.

III. FIELD OF STRESSES.

Stresses are the derivatives of the free energy with respect to the strains, $\sigma_{ij} = \partial\mathcal{F}_s/\partial u_{ij}$,

$$\sigma_{xx} = \frac{3}{4}(\partial_u u_u + \partial_w u_w) - 3W, \quad (6a)$$

$$\sigma_{xy} = \frac{\sqrt{3}}{4}(\partial_w u_w - \partial_u u_u), \quad (6b)$$

$$\sigma_{yy} = \frac{1}{4}(\partial_u u_u + \partial_w u_w) + \partial_v u_v - 3W. \quad (6c)$$

The same equations, but for a constant factor, would have been obtained if instead of Eq. 3, Eq. 1 had been used. This is a result that enhances the goodities of the triangular symmetry in the description of homogeneous media. Eqs. 6 are evaluated at each node of the system, considering the partial derivatives as finite differences of the displacements of the neighbor connected nodes.

To illustrate the capabilities of the method, two different stress conditions that lead to a straight crack are shown in Fig. 3. Both system sizes are 30×100 . The shading correspond to dividing the set of stresses in 10 greys, and putting the same amount of points in each color. This is done to see more clearly the symmetries in each component of the stress tensor, and the differences between the two drivings. The frames are taken when the crack tip is in the middle of the plate. The stress driven plate is simulated by applying forces at each boundary node such that $\sigma_{xx} = \sigma_0$, and $\sigma_{xy} = \sigma_{yy} = 0$, when there are no springs cut from the plate. Temperature now is constant (zero). For the stress driven plate, the stress of the crack tip grows as crack evolves, where probably the cuasistatic description used here fails due to the acceleration of fracture. Nevertheless, qualitatively, the stress profiles shown in Fig. 3 must remain the same in a dynamic description of the problem.

As seen from Fig. 3 the symmetries in the stress tensor for the thermally driven fracture are more complicated than for the stress driven one. Symmetries of different stresses that can be also found by analytically solving the equations for the Airy function [16], obtaining results consistent with the simulations.

To take a closer look to the crack tip divergence, sections along the middle of the plate are drawn in Fig. 4, where σ_{xy} is not plotted, as is, by symmetry, zero, or, numerically, very close to zero due to effects of the small lattices considered. Unfortunately the divergence of the stresses near the crack tip consist only of a couple of data points that are not enough to determine the exponents of the divergence.

IV. SIZE DEPENDENCE.

One of the objections that may be argued about last section is that the size of the cracks shown was too small to get any detail of questions of fundamental importance like stress

divergence at the tips, or even the location of the tip itself. As we are treating a model that is but a mere discretization of the elastic equations, if all the lengths of a given simulation (system size, ξ , and $l_T = 1/v$), were scaled by a factor, the new simulation would reproduce, at larger scale, the patterns obtained in the small scale one (and much less CPU consuming one). But be forgot to rescale the stress threshold σ_{th} , that has really units of stress divided by length.

To guess this scaling we will follow an argument also used in effective medium theories for elastic percolation [17]. We can apply a force of modulus f , pulling two nodes of the triangular lattice apart. It would produce a displacement proportional to f , and the proportionality constant is the effective spring constant in the system, $1/a^*$, due to all possible connections of the two nodes through the infinite triangular lattice [18]. As σ_{th} takes in account only the direct connection between neighbor nodes, the contribution of the medium must be subtracted. The expression for the threshold stress, when the lengths of the system are multiplied by n , is given, in this approximation, by

$$\sigma_{th}^{(n)} = \frac{n}{a_n^*} - \left(\frac{1}{a_1^*} - 1 \right), \quad (7)$$

where a_n^* is calculated putting the force f n nodes apart in one of the directions of the triangular lattice.

Eq. 7 turns out to be only a good approximation (really an upper bound) to the value that rescales the system to find the same crack patterns reproduced. Fig. 5 shows such rescaling for one of the cracks shown in Fig. 2. The shape (wavelength and amplitude) are the same for the three discretizations, but the threshold stresses are not exactly those given by Eq. 7 (changes in σ_{th} are translated to changes in ΔW since in the simulations the convention is that $\sigma_{th} = 1$). For size 60×200 (90×300), $\sigma_{th} = 1.452(1.8)$ in Fig. 5, and from Eq. 7 we would have that $\sigma_{th} = 1.475(1.952)$, values that lead to a straight crack in the simulations.

Thus, the theoretical values for σ_{th} obtained by this method are not the right ones [19], but provide a good estimation that can save time when we want to have larger systems and we do not want to sweep the hole parameter space involving large simulations. As a reference, the 90×300 crack presented here took 5 days cpu time in an alpha machine.

V. CONCLUSIONS.

As conclusions, we have seen that hookean springs placed in a triangular lattice, and coupled to the temperature defined at each node, provides a discrete model for simulating brittle materials, in agreement with the behavior of continuum elasticity theory. Simulations reproduce qualitatively well experiments, but still, a simple description from a theoretical point of view is missing. The simulation framework presented here can provide a valuable tool to check new proposals for explaining fracture phenomena. Some possible extensions of this work follow.

Here we have analyzed the case in which all the springs have the same force constant, or in the elastic language $\lambda = \mu$. This is not the case for most materials. In order to simulate materials with different ratios in the Lamé coefficients a $\sqrt{3} \times \sqrt{3}$ reconstruction of the triangular lattice with two different force constants may be used [20].

It is also tempting to think of this thermally activated cracking effect as a basis of a machinery that could microfabricate all kinds of devices. By passing the glass film in one direction through the thermal gradient, and then backwards in the other, and also modifying the intensity of the temperature change, a large variety of forms can be achieved, and all with relatively high accuracy.

The extension of the calculations done in this work to two dimensional disks is not difficult. The question is if this kind of fracture can be accomplished experimentally.

Another problem of technological interest for which very similar techniques to those employed here is stress corrosion cracking. In this case a poisoning agent plays the role of temperature by increasing locally the volume of the material (the scalar field that couples to elastic displacements is concentration).

ACKNOWLEDGMENTS

I am in debt with Paco Guinea for introducing me to the subject, and for his encouragement and discussions through this work. I also acknowledge financial support from the spanish CICYT Grant MAT94-0982-C02-02, and useful discussions with Enrique Louis and Shu-zhu Zhang.

REFERENCES

- * E-mail oscar@quijote.icm.uam.es.
- [1] B. Lawn, “Fracture of Brittle Solids”, (Cambridge University Press, Cambridge, 1993).
 - [2] “Disorder and Fracture”, J. C. Charmet et. al eds. (NATO ASI Series vol. 235, Plenum Press, New York, 1990).
 - [3] M. Sahimi and S. Arbabi, Phys. Rev. B, **47**, 713 (1993) and references therein.
 - [4] A. Yuse and M. Sano, Nature **362**, 329 (1993).
 - [5] M. Marder, Phys. Rev. E, **49**, R51 (1994)
 - [6] S. Sasa, K. Sekimoto and H. Nakanishi, Phys. Rev. E, **50**, R1733 (1994).
 - [7] Y. Hayakawa, Phys. Rev. E, **49**, R1804 (1994).
 - [8] Y. Hayakawa, Phys. Rev. E, **50**, R1748 (1994).
 - [9] F. F. Abraham, D. Brodbeck, R. A. Rafey, and W. E. Rudge, Phys. Rev. Lett., **73**, 272 (1994).
 - [10] L.D. Landau and E.M. Lifshitz, “Theory of elasticity”, (Pergamon, New York, 1959).
 - [11] Since terms in the free energy that depend only on the scalar field W will not contribute to the stresses nor the equilibrium equations of the displacements, Eq. 2 could have been written as $\mathcal{F}_s = \sum_{i \neq j} k_{ij} [(\mathbf{u}_j - \mathbf{u}_i) \hat{r}_{ij} - (W_i + W_j)/2]^2$. This could have the interpretation of changing the equilibrium distance of the spring from 1 to $1 + (W_i + W_j)/2$, as done in previously proposed discrete models [7,8].
 - [12] Note that this reference system is not orthogonal, but the election makes easier to work with triangular lattices.
 - [13] For a general description of Conjugate Gradients Method, see, for instance, “Numerical Recipes”, W. H. Press, B. P. Flannery, S. A. Teutolsky, and W. T. Vettering (Cambridge University Press, Cambridge, 1986).
 - [14] E. Louis and F. Guinea, Europhys. Lett. **3**, 871 (1987); Physica D **38**, 235 (1989).
 - [15] P. Meakin, G. Li, L. M. Sander, E. Louis, and F. Guinea, J. Phys. A, **22**, 1393 (1989).
 - [16] V. Hakim, private communication.
 - [17] S. Feng, M. F. Thorpe, and E. Garboczi, Phys. Rev. B, **31**, 276 (1985).
 - [18] The explicit calculation is done by expressing the fourier transform of the displacements as product of minus the dynamical matrix times the fourier transform of the applied forces, $u_k = -D(k)F_k$. And back to real space integrating over the Brillouin zone of the triangular lattice. For more details see [17].
 - [19] The theoretical values of σ_{th} can get closer to those found euristically in the simulations by including the finite size of the plates on the modification of the Brilluin zone, but still do give straight cracks for large change of system size. A more detailed calculation should involve all possible paths of stresses throug the system, and may be the implicit consideration of the temperature.
 - [20] O. Pla, R. Garcia-Molina, F. Guinea, and E. Louis, Phys. Rev. B, **41**, 11449, (1990).

FIGURES

FIG. 1. On the left, schematic representation of Yuse and Sano experiment. The right part shows the temperature profile in the system (see text).

FIG. 2. Simplified phase space showing straight, oscillating and several levels of branching for systems of size 30×100 and $\xi = 6$.

FIG. 3. Stresses in the plate, for two different stress conditions that give rise to a straight crack: in the upper part thermally driven with $\Delta W = 1.8$, $\nu = 1$, and $\xi = 6$; and in the lower part uniform uniaxial stress in the x -axis ($\sigma_0 = 1.5$). Both profiles were taken when the crack is at the middle of the plate. System sizes are, for both cases, 30×100 .

FIG. 4. Cross section of the stresses shown in Fig. 3 along the crack.

FIG. 5. One of the wiggling crack patterns of Fig. 2 ($\Delta W = 1.8$, and $\nu = 3$), and scaling it for twice and three times the involved lengths. For twice $\Delta W = 1.24$, and for three times $\Delta W = 1.0$.

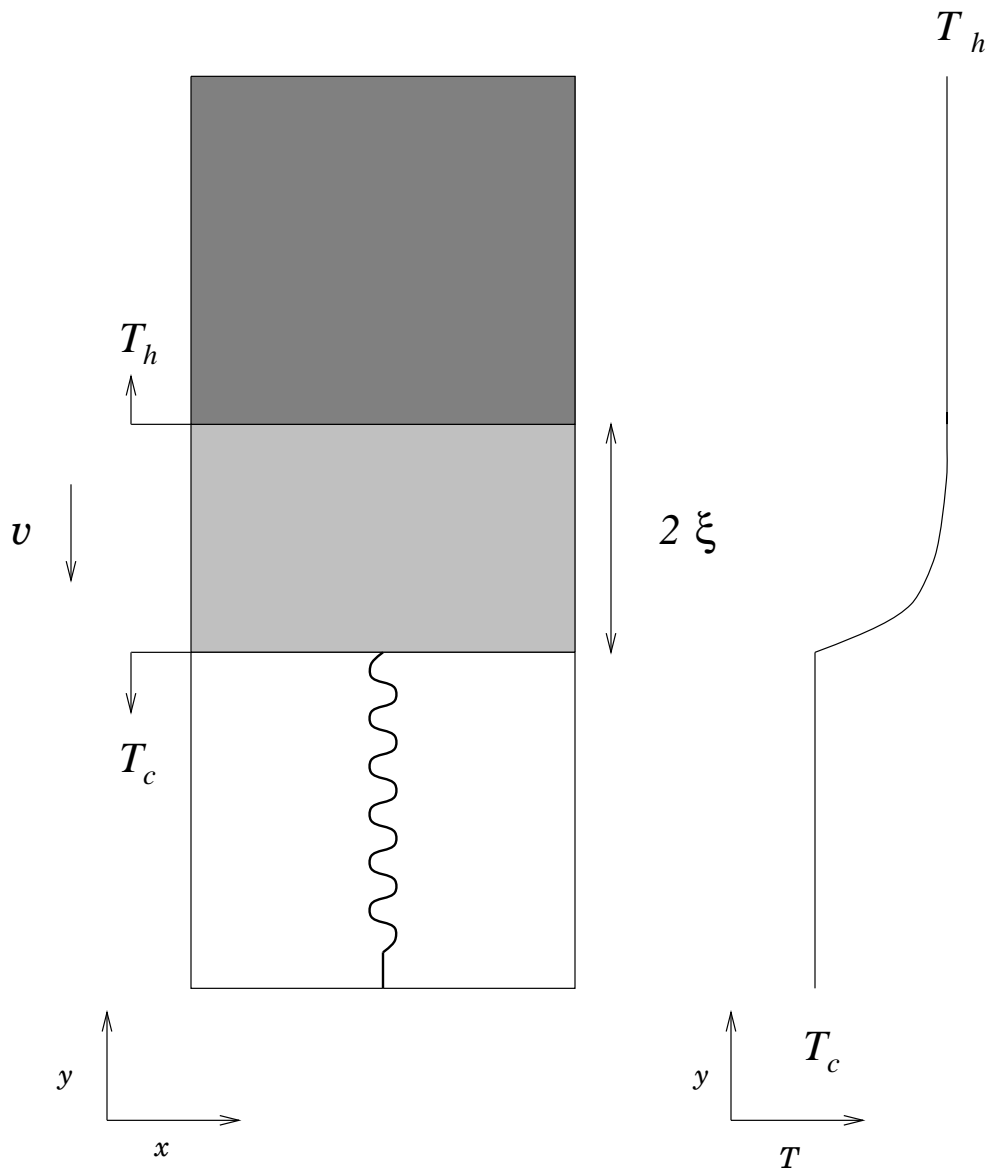


Figure 1, O. Pla

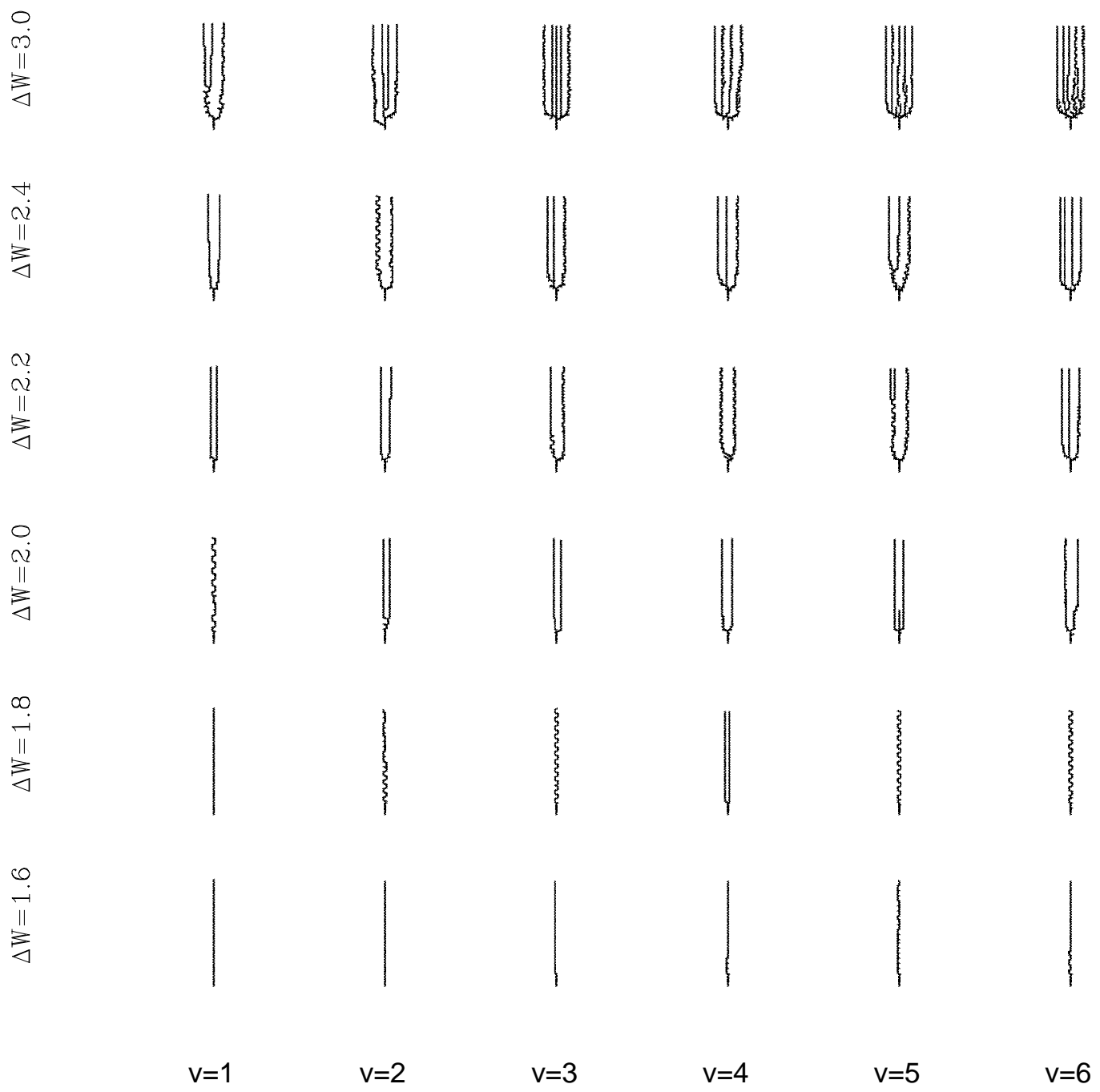
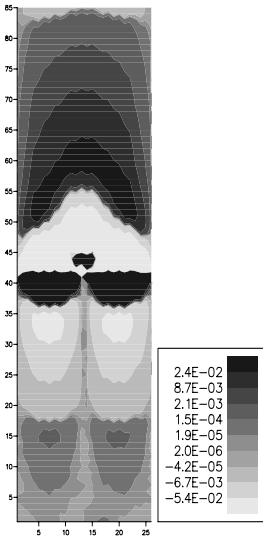
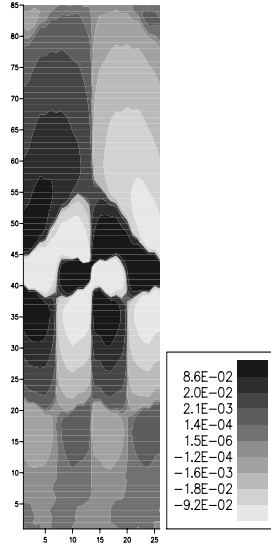


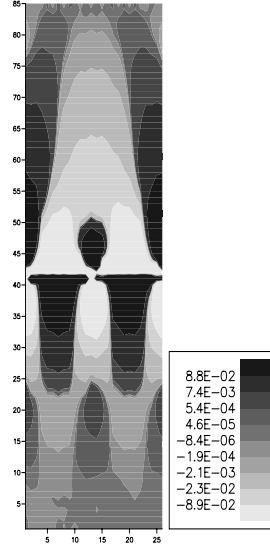
Figure 2, 0. Pla



σ_{xx}



σ_{xy}



σ_{yy}

*Thermally
driven*

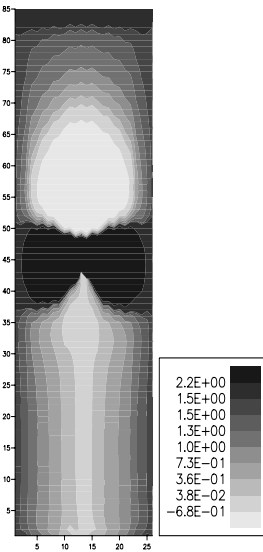
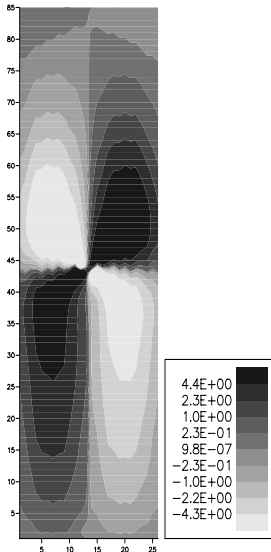
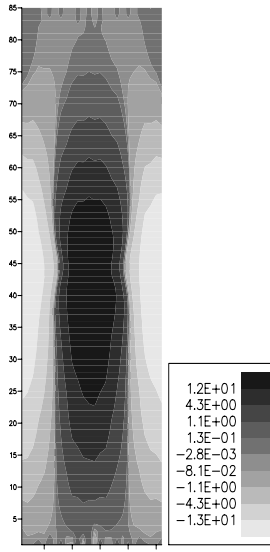
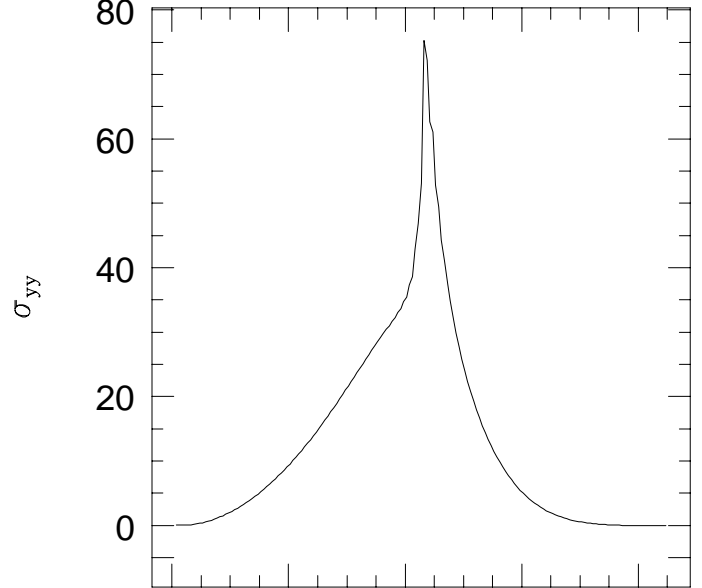
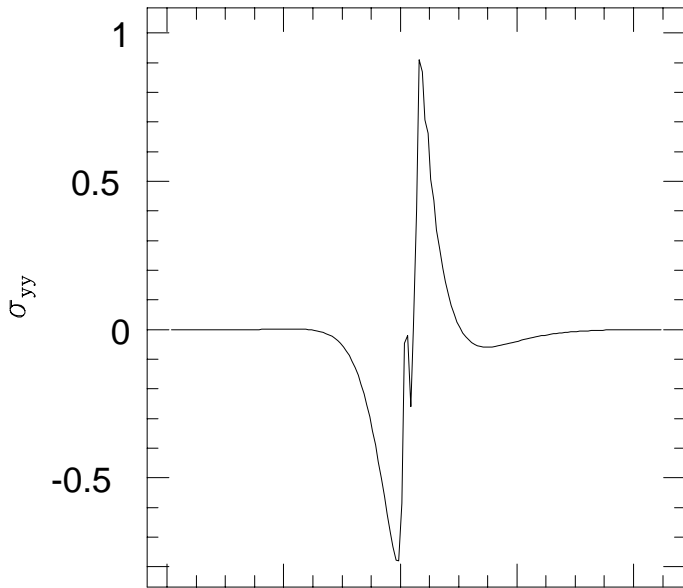
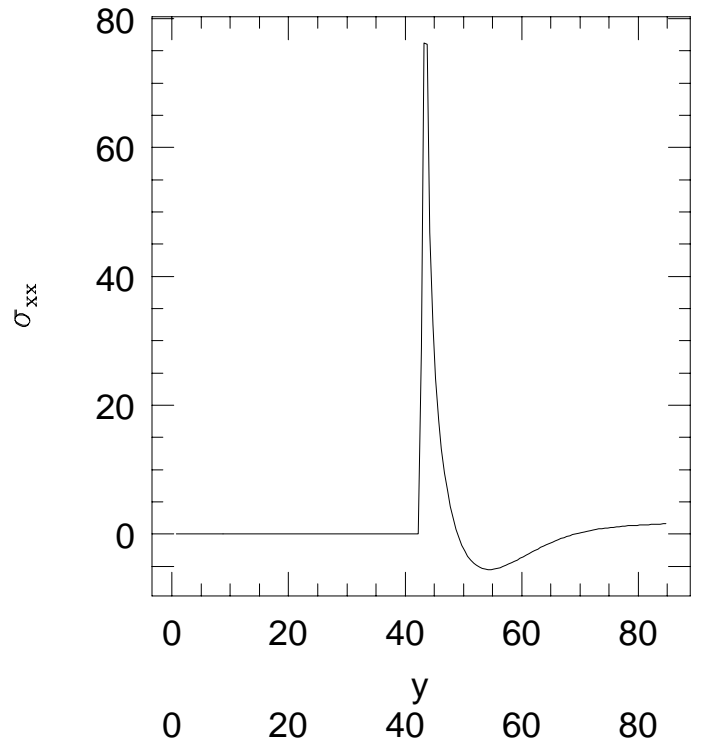
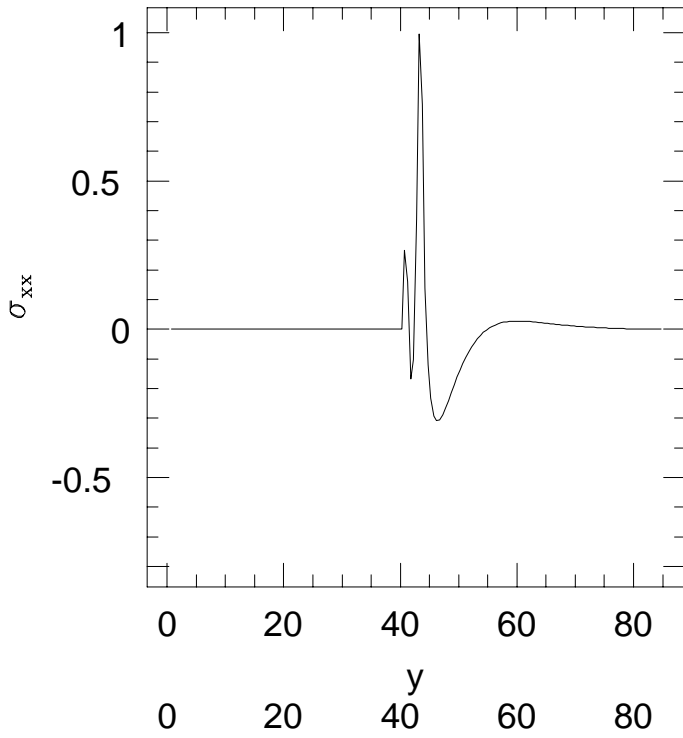


Figure 3, 0. Pla



*Stress
driven*





Thermally driven

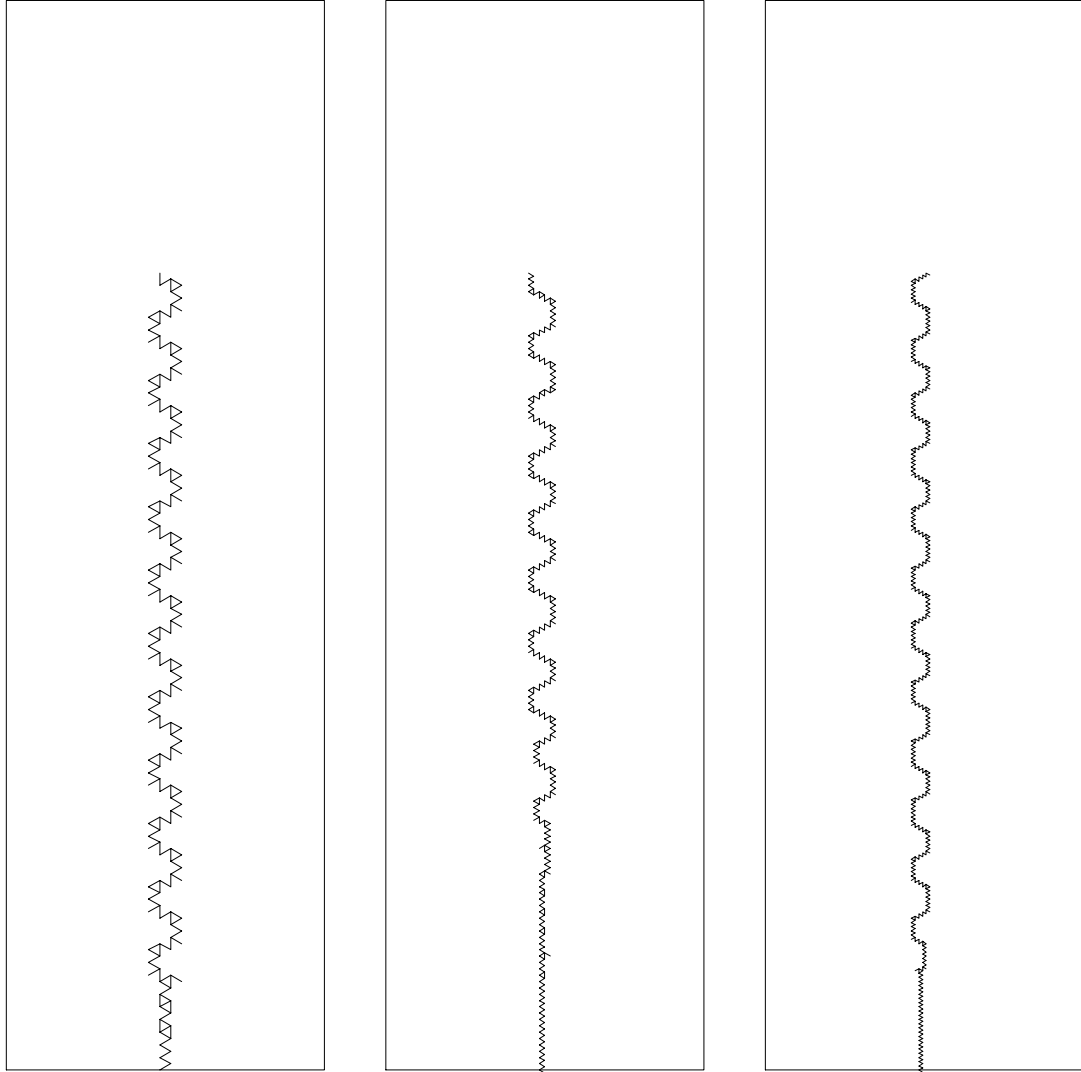
Stress driven

Figure 4, O. Pla

$\Delta W=1.8$

$\Delta W=1.24$

$\Delta W=1.0$



30x100

60x200

90x300

Figure 5, 0. Pla